Basic Characteristics of Implantable Flexible Pressure Sensor for Wireless Readout using MRI

Tatsuya Nakamura, Yusuke Inoue, Dongmin Kim, Naoji Matsuhisa, Tomoyuki Yokota, Tsuyoshi Sekitani, Takao Someya, *Member, IEEE,* Masaki Sekino, *Member, IEEE*

***Abstract*—Measuring the local pressure in blood vessels is valuable in the postoperative monitoring of aneurysms. However, implanting a conventional pressure sensor equipped with power and signal cables causes difficulties during the operative procedure and carries a risk of infection after the implantation. In this study, we developed a wireless, implantable, and flexible pressure sensor. A magnetic resonance imaging (MRI) system reads out the sensor output. The proposed wireless sensor is based on an LC resonant circuit with a spiral coil and a pressure-sensitive capacitor. The pressure-dependence of the capacitance affects the magnetic field produced by the spiral coil, changing the magnetization of the nearby sample that can be observed as a signal variation by MRI. We fabricated a prototype sensor using a capacitor with a silicone elastomer as the dielectric and a spiral coil made of gold. The maximum change in the capacitance was 8% under an external pressure of 20 kPa. A change in the thickness of the dielectric elastomer caused the capacitance to change, resulting in a signal variation detectable by MRI.**

I. Introduction

Measuring the local pressure in small internal body structures, such as blood vessels, intracranial space, and joints, is essential for detecting physiological abnormalities in the human body. However, implanting conventional pressure sensors, which are equipped with power and signal cables, causes difficulties during the surgical procedure and increases the risk of postoperative infection. Therefore, wireless transmission of signals and power is a desirable feature of implanted pressure sensors. A few wireless pressure sensors have been developed; however, there are difficulties either in measuring the pressure in deeper parts of the human body by a sensor or in distinguishing multiple sensors that are implanted [1][2].

One of the diseases that necessitates the use of wireless pressure sensors is an aneurysm. The main treatment of this disease is the insertion of a stent graft. The inserted stent graft protects the blood vessel wall from being damaged by blood pressure, eliminating the risk of a rupture. This procedure sometimes fails when the stent graft is warped or displaced and the aneurysm is still pressurized [3]. Routine postoperative monitoring is carried out for confirming the proper functioning of stent grafts. Presently, computed tomography (CT) scans are performed for monitoring in many cases, but by this method, the stent graft can only be morphologically observed and the leakage of blood cannot be detected. Blood leakage could be detected if a small wireless pressure sensor is implemented on the surface of the stent graft.

In this study, we developed a pressure sensor whose circuit characteristics change depending on the external pressure. The sensor consists of a pressure-sensitive capacitor and a coil, forming a resonance circuit. Wireless readout is achieved using an MRI system. The sensor detects a pressure of 20 kPa, which corresponds to blood pressure.

II. Principle and Fabrication of the Sensor

The proposed sensor is based on an LC resonance circuit with a spiral coil and a pressure-sensitive capacitor (Fig. 1). The radio frequency (RF) coil in an MRI system applies an RF magnetic field that passes through the spiral coil. The application of the RF fields induces electric currents in the circuit. The dielectric in the capacitor has elasticity, which—when changed by an externally applied pressure—causes a change in the capacitance. The pressure-dependent circuit affects the magnetic field produced by the current flowing in the spiral coil. The generated field affects the magnetization of nearby samples that can be observed as an MRI signal variation.

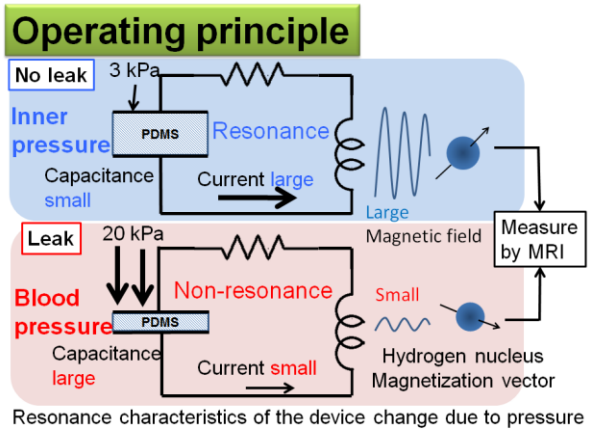

Figure 1. Operating principle of the proposed pressure sensor based on an LC resonant circuit. External pressure affects the gap between the polar plates in the capacitor.

A. Device design

The LC resonance circuit was designed to resonate at the frequency of 300 MHz, which was equal to that of the RF magnetic fields in our MRI system. To use this sensor inside the human body, it is necessary to design the sensor as small as possible and to give mechanical flexibility. We set the coil inductance as 161 nH and the capacitance as 1.75 pF. Table I lists the parameters of the spiral coil and the capacitor. We used polydimethylsiloxane (PDMS) as the dielectric elastomer

Tatsuya Nakamura, Yusuke Inoue, Dongmin Kim, Naoji Matsuhisa, Tomoyuki Yokota, Tsuyoshi Sekitani, Takao Someya, and Masaki Sekino are with the Department of Electrical Engineering and Information Systems, Graduate School of Engineering, the University of Tokyo, Tokyo 113-8656, Japan, and also with the Exploratory Research for Advanced Technology (ERATO), Japan Science and Technology Agency (JST), Tokyo 113-0032, Japan. (e-mail: nakamura@bee.t.u-tokyo.ac.jp; someya@ee.t.u-tokyo.ac.jp; sekino@bee.t.u-tokyo.ac.jp)

978-1-4244-7929-0/14/$26.00 ©2014 IEEE

because of its biocompatibility, changeable Young's modulus, and adaptable thickness. Fig. 2 (a) shows the fabrication process and structure of the sensor.

TABLE I. PARAMETERS OF THE SPIRAL COIL AND CAPACITOR

External diameter	10.0 mm
Internal diameter	3 mm
Number of turns	5 times
Width of conductor	0.2 mm
Inductance	308 K
Size of polar plate	3 mm × 3 mm
Gap between polar plates	125 μm
Capacitance	1.75 pF

B. Fabrication Process

The principal processes used to fabricate the sensor were gold evaporation and PDMS spin coating. The device consisted of three layers. The spiral coil was patterned on the first layer, and the second layer had the PDMS dielectric. The third layer contained a polar plate of the capacitor (Fig. 2 (a)).

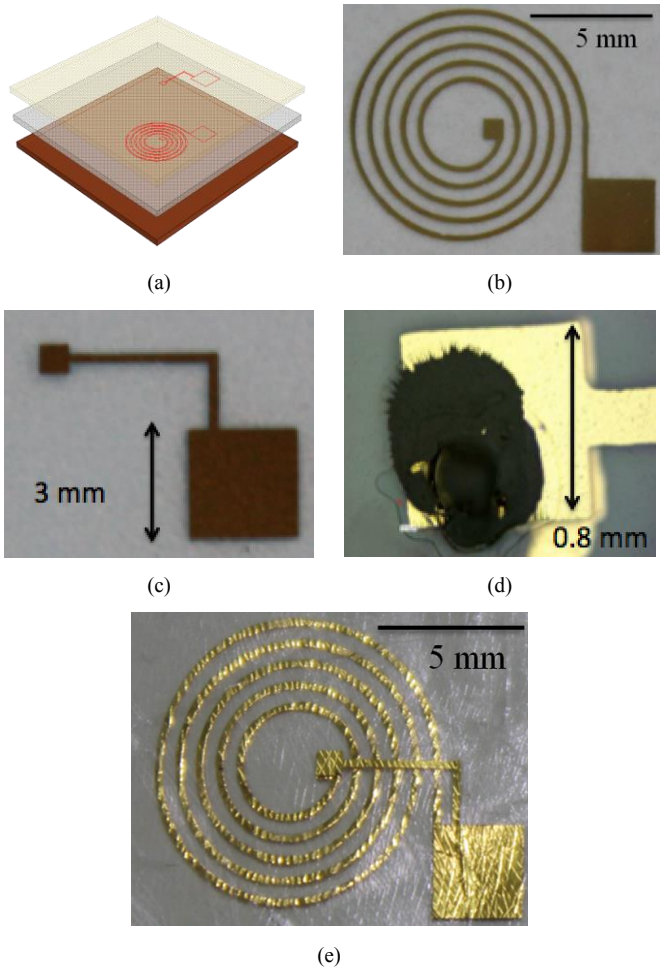

Figure 2. Detailed fabrication process of the sensor. (a) The device consisted of three layers. (b) A spiral coil was patterned on the first layer. (c) The third layer had a polar plate of the capacitor. (d) A via hole at the center of the spiral coil connected the first and third layers. The hole was filled with black conductive paste. (e) The fabricated device.

Gold was evaporated on a thin plastic film to make the spiral coil and one polar plate of the capacitor (b). The first layer was soaked in PDMS with its mixing rate controlled, and the second layer was formed using spin coating. We then patterned the paired polar plate on another plastic film (c), and pasted it on the PDMS dielectric (e). The electrical connection between the first and third layers was achieved by making a via hole at the center of the coil using a CO_2 laser and filling the hole with a conductive paste (d).

III. EXPERIMENTS

A. Pressure–Capacitance Characteristics

To investigate the pressure–capacitance characteristics, we measured the capacitance, moving the polar plate uniformly by applying a given weight. We fabricated a 2 cm^2 capacitor by filling PDMS as the dielectric between the two polar plates, and set its thickness as 116 μm. With the setup shown in Fig. 3(a), the capacitance was measured using an LCR meter.

B. Change in LC Resonance Characteristics

Three sensors having PDMS thicknesses of 44, 66, and 170 μm were fabricated, and the LC resonance characteristics were measured for each of them. We measured the absolute value of impedance at frequencies ranging from 10 MHz to 300 MHz using a network analyzer. A pair of electrode pads was additionally patterned on the sensor to facilitate measurement by attaching the pads to the probes of the network analyzer.

C. Evaluation of Flexibility

We fabricated the sensor on a 1.4 μm PET film substrate to evaluate the mechanical flexibility of the sensor. The frequency characteristics were measured under two conditions: when the device was folded, and when it was flat. The sensor was attached on an acrylic rod whose diameter (15 mm) was equal to that of the aorta (Fig. 3 (b)). We measured the absolute value of impedance at frequencies ranging from 10 MHz to 300 MHz.

D. Acquisition of MRI

MRI was used to observe the spatial distribution of magnetic fields generated by the flow of current in the spiral coil. The experiments were carried out using a 7T MRI system. We obtained MRI under two different conditions, and estimated the induced magnetic fields from the images. At first, an RF preparation pulse for making the sample magnetization vector flip by $\pi/3$ was irradiated. This was followed by irradiation of a pulse for making the magnetization flip by $\pi/6$. Under this condition, we took the first MRI. Next, the RF pulse for making the magnetization flip by $\pi/6$ was solely irradiated, and the second MRI was taken. By analyzing these two images, we estimated by how many angles the magnetic vector flipped the magnetization and how strong was the induced magnetic field (Fig. 4). We compared the results with the simulated data. The simulated data provided the intensity distribution of the RF signal at 1 mm above the surface of the pressure sensor.

E. Intensity Distribution of RF Fields in MRI Acquisition

We performed MRI of the prototypes fabricated with different PDMS thicknesses. The sensors were placed in agar (Fig. 3 (c)), which is the most commonly used medium to model biological tissues.

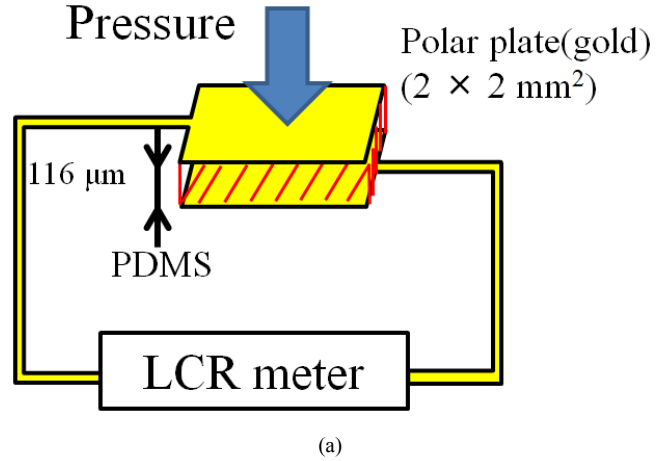

(a)

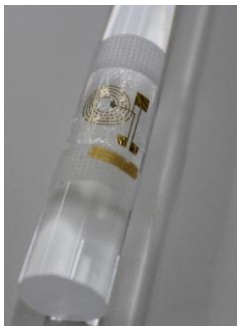

(b)

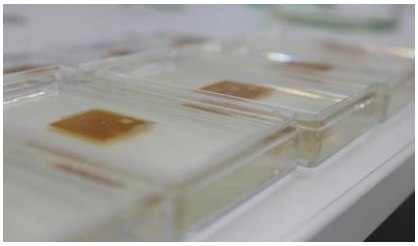

(c)

Figure 3. Experimental methods for evaluating the pressure-sensitivity and flexibility. (a) Circuit characteristics were measured using an LCR meter with an external pressure applied on the capacitor. (b) The device is contoured to conform to a rod, showing that the device can be attached on a stent graft. (c) The device was immersed in agar for MRI acquisition.

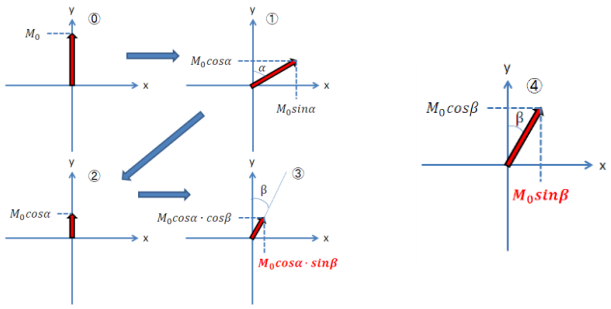

Figure 4. Method for mapping the magnitude of RF magnetic fields of MRI around the sensor. Images were obtained with and without applying an RF preparation pulse of a flip angle α, resulting in the respective signal intensities of $M_0 \cos\alpha$. $\sin\beta$ and $M_0 \sin\beta$. A comparison of these two images gives an estimate of the magnitude distribution of the preparation pulse.

IV. Results and Discussion

A. Pressure–Capacitance Characteristics

The pressure–capacitance characteristics measured using an LCR meter are shown in Fig. 5. The maximum variation in the capacitance was 8% under the external pressure of 20 kPa, and the capacitance changed by 3.3% when pressure changed from 3 kPa to 20 kPa. The elastomer exhibited critical strain at approximately 7 kPa. Because of the relatively small variation in the capacitance, the readout of pressure based on the resonance frequency is effective.

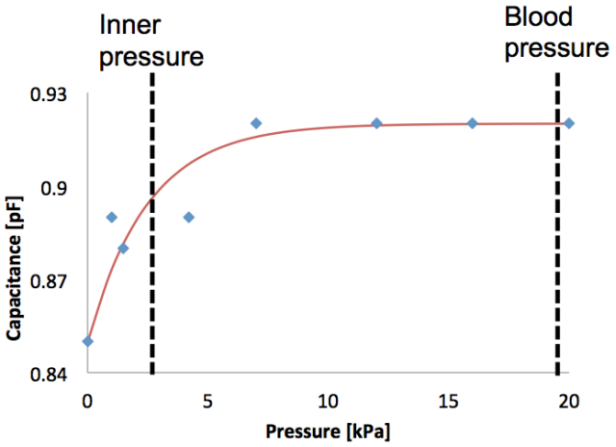

Figure 5. Pressure–capacitance characteristics. The capacitance shows a detectable variation when measured at the inner body pressure and the blood pressure.

B. Change in LC Resonance Characteristics

The fabricated pressure sensor was composed of the LC resonance circuit with the spiral coil, and its frequency characteristics were observed to change with the variation in PDMS thickness. Fig. 6 and Table II show the measured frequency characteristics and the resonant frequency, respectively. The frequency of the RF field is proportional to the strength of the static magnetic field, depending on individual MRI systems. The results indicate that the resonant frequency of the device can be adjusted to suit the frequency of the MRI system. Considering the prevailing use of 1.5 T (64 MHz) MRI for clinical investigation, setting the resonant frequency to 64 MHz would be useful.

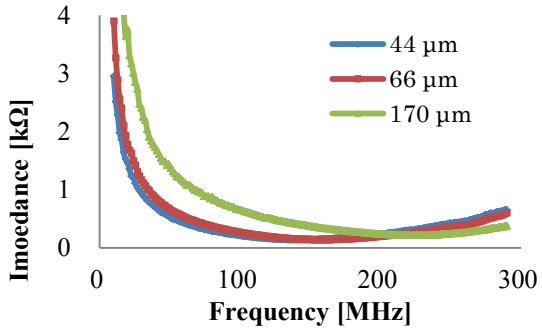

Figure 6. Frequency characteristics of the device impedance, with varied gap between the polar plates in the capacitor.

TABLE II. Dependence of the Resonant Frequency on the Thickness of the Dielectric

PDMS thickness [μm]	44	66	170
Resonance frequency [MHz]	165	180	>300

C. Evaluation of Flexibility

The frequency characteristics were measured with the sensor attached both on a flat plate and on a curved surface. We observed that the frequency–impedance characteristics of the pressure sensor did not change much, as shown in Fig. 7.

This low sensitivity of sensor characteristics to the geometry would be beneficial when the sensor is attached on the surface of implants, which may have curved or flexible surfaces.

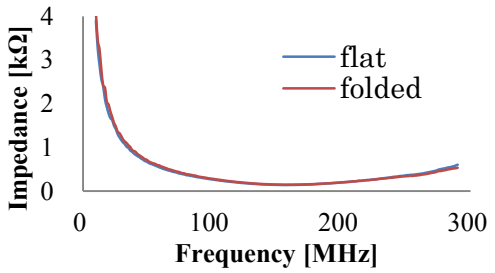

Figure 7. Frequency characteristics of the pressure sensor. The measurements were carried out with the sensor fixed on a flat surface and on a curved surface.

D. Intensity Distribution of RF Fields in MRI Acquisition

The experimental results exhibited spatial variations similar to the theoretical estimated values of the induced magnetic field, as shown in Fig. 8 [4][5][6]. The green curve shows the simulation result, whereas the red and blue plots show the measured results of the device under off-resonance and resonance conditions, respectively. Magnetic field strength in resonant device increased as it approached center of the coil, while that of off-resonant device decreased.

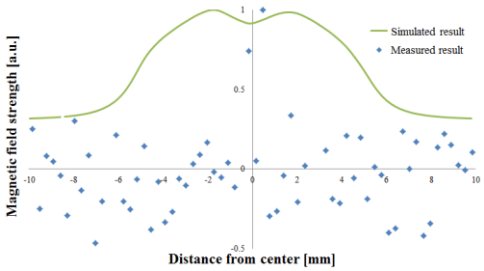

(a) Theoretical estimation and experimental results of the strength of the RF magnetic field generated by the resonant device.

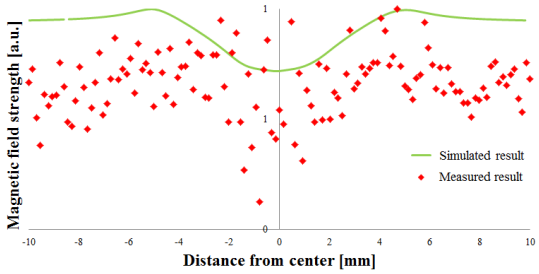

(b) Strength of the RF magnetic field generated by the off-resonant device.

Figure 8. Distribution of RF fields around the pressure sensor.

E. Acquisition of MRI

Magnetic resonance images were obtained for the three prototype devices which is only coil and are having different thicknesses of the dielectric elastomer (100µm and 400µm), as shown in Fig. 9. The signals were generated mainly from the surrounding agar. The condenser and PDMS thickness affected the generated magnetic fields and resulting images. The results show the possibility of reading out the pressure variation using MRI.

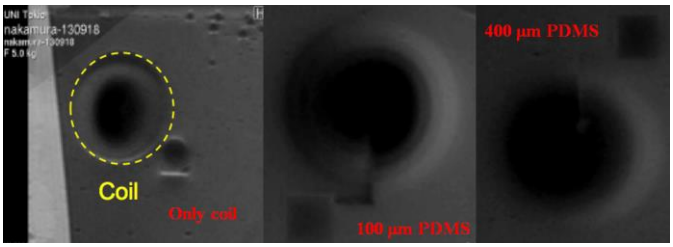

Figure 9. Magnetic resonance images of the sensor. The sensor was embedded in agar. Condenser and Variation in the dielectric thickness affects the MRI signals.

This paper proposed the readout of pressure using MRI. Other options do exist for applying external magnetic fields to the sensor and detecting a variation in the resonant frequency. However, the advantages of using MRI are that it allows for multi-point readout and implantation deep inside the body. MRI can also distinguish individual sensors when multiple sensors situated close to each other are used. In addition, MRI can selectively sense the variation in RF magnetic fields in close proximity to the sensor.

V. Conclusions

In this study, we proposed an implantable flexible pressure sensor, and established its fabrication process. Changing the resonant characteristics of the sensor resulted in the variation of MRI signals in close proximity to the sensor. The sensitivity of the device was confirmed to be sufficiently high for detecting the blood pressure. Bending of the sensor hardly affected the circuit characteristics, showing the feasibility of implementation on the surface of implantable medical devices.

Our next steps are to further improve the pressure-sensibility of the capacitor [7][8], and to obtain images using MRI when the pressure sensor is attached on a stent graft.

References

[1] M. A. Fonseca, M. G. Allen, J. Kroh, J. White, "Flexible wireless passive pressure sensors for biomedical applications," *Solid-State Sensors, Actuators, and Microsystems Workshop,* June 4–8, (2006).

[2] P-J. Chen, S. Saati, R. Varma, M. S. Humayun, Y-C. Tai, "Implantable flexible-coiled wireless intraocular pressure sensor," *IEEE*, (2009).

[3] R. K. Greenberg, T. A. M. Chuter, R. P. Cambria, W. C. Sternbergh III, N. E. Fearnot, "Zenith abdominal aortic aneurysm endovascular graft," *Journal of Vascular Surgery*, 48(1), pp. 1–9, (2008).

[4] D. I. Hoult, PhD, "The principle of reciprocity in signal strength calculations-A mathematical guide," *Concepts in Magnetic Resonance*, 12(4), pp. 173-187, (2000).

[5] D-J. Guo, S-J. Xiao, H-B. Liu, B. Xia, J. Wang, J. Pei, Y. Pan, Z-Z. Gu, X-Z. You, "Diffusion of hydrosilanes from the control layer to the control layer to the vinylsilane-rich flow membrane during the fabrication of microfluidic chips," *Langmuir*, 21(23), pp.10487–10491, (2005).

[6] J. Pauly, D. Nishimura, A. Macovski, "A k-Space analysis of small-tip-angle excitation," *Journal of Magnetic Resonance*, 81, pp. 43–56, (1989).

[7] K. F. Lei, K-F. Lee, M-Y. Lee, "Development of a flexible PDMS capacitive pressure sensor for plantar pressure measurement," *Microelectronics Engineering*, 99, pp. 1–5, (2012).

[8] S. C. B. Mannsfeld, B. C-K. Tee, R. M. Stoltenberg, C. V. H-H. Chen, S. Barman, B. V. O. Muir, A. N. Sokolov, C. Reese, Z. Bao, "Highly sensitive flexible pressure sensors with microstructured rubber dielectric layers," *Nature Materials*, 9, pp. 859–864, (2010).